

Novel Ag⁺-Zeolite/Polymer Mixed Matrix Membranes with a High CO₂/CH₄ Selectivity

Yi Li and Tai-Shung Chung

Dept. of Chemical and Biomolecular Engineering, National University of Singapore, Singapore 119260

Santi Kulprathipanja

UOP LLC, Des Plaines, IL 60017

DOI 10.1002/aic.11109

Published online January 29, 2007 in Wiley InterScience (www.interscience.wiley.com).

A novel silver ion-exchange treatment of zeolite was introduced in this work to change the physical and chemical adsorption properties of penetrants in the zeolite. EDX data confirm the complete replacement of sodium ion in zeolite NaA by silver ion, whereas XRD patterns and BET results show no changes in some physical properties of zeolite after the silver ion-exchange treatment. Polyethersulfone (PES)-zeolite NaA mixed matrix membranes (MMMs) and PES-zeolite AgA MMMs were fabricated at high processing temperatures with different zeolite loadings. Cross-sectional SEM images of these two types of MMMs indicate the interface between polymer and zeolite phases is comparable before and after the silver ion-exchange treatment. The effects of silver ion-exchange treatment of zeolite and zeolite loadings on the gas separation performance of these MMMs were investigated. CO₂ permeability of PES-zeolite AgA MMMs is higher than that of PES-zeolite NaA MMMs, whereas their CH₄ permeability is lower than that of PES-zeolite NaA MMMs. This trend is the result of the reversible reaction between silver ion and CO₂ molecule. CO₂ and CH₄ permeability of PES-zeolite AgA MMMs decreases with increasing zeolite content arising from the effects of partial pore blockage of zeolite and polymer chain rigidification, whereas their CO₂/CH₄ selectivity increases with an increase in zeolite loadings and the highest value reaches 59.6 at 50 wt % zeolite loading because of a combined effect of the facilitated transport mechanism of silver ion and the molecular sieving mechanism of zeolite. Both CO₂-induced plasticization test and CO₂/CH₄ mixed gas measurement were performed to examine the applicability of these developed PES-zeolite AgA MMMs in industry. Results prove that this type of composite membrane material is a superior candidate for the practical separation of natural gas. © 2007 American Institute of Chemical Engineers AIChE J, 53: 610–616, 2007

Keywords: silver ion-exchange treatment of zeolite, mixed matrix membranes (MMMs), natural gas separation, facilitated transport mechanism, molecular sieving mechanism

Introduction

The separation of carbon dioxide from methane in the process of natural gas and landfill gas treatment is essential to reduce pipeline corruptions induced by acid CO₂ gas as well as to produce high-purity energy products.^{1–4} To meet pipeline requirements, CO₂ must comply with such a concentra-

tion specification as <2%. Available techniques for natural gas separation include membrane, absorption, adsorption, and cryogenic distillation. Membrane processes have been proven to be technically and economically superior to other competing technologies in many industrial applications. This superiority is explained by many advantages of membrane separation technology, which include low capital investment, simplicity and ease of installation and operation, low maintenance requirements, low weight and space requirements, and high process flexibility. A type of successful membrane material for natural gas separation should possess

Correspondence concerning this article should be addressed to T.-S. Chung at chencts@nus.edu.sg.

the following characteristics: (1) inherently high permselectivity for CO₂ and CH₄ gas pair and (2) immunity to plasticization induced by CO₂. The CO₂-induced plasticization usually results in a severe deterioration of membrane separation performance.

However, the practical application of membranes made from neat polymer materials has been constrained by a performance “upper bound” limit of the permeability–selectivity relationship.⁵ To extend the industrial applications of membrane separation technology, it is essential to synthesize and develop high-performance membrane materials. The facilitated transport membrane technique is one of various synthetic methods for natural gas and hydrocarbon separation where the membrane materials are incorporated with such noble metal ions as Ag⁺ or Cu⁺.^{6–9} CO₂ and hydrocarbon gases with double bonds can react reversibly with these noble metal ions and form a π -bonded complex, thus obtaining a high separation performance. The most commonly used facilitated transport membrane types are (1) immobilized liquid membranes; (2) solvent swollen, fixed-site carrier membranes; and (3) solid electrolyte polymer. Although these facilitated transport membranes have shown very high performance with respect to natural gas and hydrocarbon separation, their mechanical and long-term high-performance stabilities are very poor, primarily because the noble metal ions are liable to be reduced to form metal nanoparticles and further aggregate to each other. Therefore, a practical application of facilitated transport membranes in natural gas separation is still pending.

After the discovery by researchers at UOP on mixed matrix membranes (MMMs),¹⁰ the latest emerging membrane materials constituting molecular sieve entities embedded in a polymer matrix provide another potential solution to surpass the “upper bound” limit of the permeability–selectivity relationship by means of combining the easy processability of polymer materials with the superior gas separation properties of molecular sieve materials.^{11–16} Progress has been made in polymer–zeolite MMMs for natural gas separation,¹⁷ which showed a significant increase in CO₂/CH₄ selectivity of roughly 44% at 50 wt % zeolite loading compared with that of neat polymer dense film. Zeolites, which are microporous crystalline materials,^{18–20} are allowed to act as molecular sieves because of their particular structure—a three-dimensional pore structure consisting of a network of interconnected tunnels and cages—and nearly uniform pore and channel sizes. Therefore, zeolites possess the ability to separate and remove one gas from a similarly sized gas mixture based on their size- and shape-selective nature. In the work done by Li et al.,¹⁷ both CO₂ and CH₄ gases possessed little or no affinity for the polymer matrix and zeolite 4A; therefore, it was the precise tailoring of pore size [3.8×10^{-10} m (3.8 Å)] of zeolite 4A that resulted in a significant increment in CO₂/CH₄ selectivity of MMMs. However, to achieve even higher separation performance, it is necessary to go beyond the tailoring of pore sizes.

It is well known that the pore size of zeolites A, X, and Y can vary by changing the cations present therein arising from the different ionic radii of exchanged cations. For example, zeolite 4A (also called NaA) includes sodium ion and has a pore size of 3.8×10^{-10} m (3.8 Å), whereas zeolites KA and CaA have pore sizes of 3×10^{-10} m (3 Å) and 4.8×10^{-10} m (4.8 Å) after sodium ion in zeolite NaA is

exchanged with potassium ion and calcium ion, respectively. This type of property has rendered the ion-exchange treatment of zeolites A, X, and Y very attractive for use in applications where the molecular sieving takes effect in the range of $3\text{--}8 \times 10^{-10}$ m (3–8 Å). However, most investigations focused primarily on the change of zeolite pore size by the ion-exchange treatment, thus influencing the diffusion properties of penetrants in the zeolite.^{21–23} Little work has been done on the exchange treatment of zeolite with noble metal ions, such as Ag⁺ and Cu⁺, to change the physical and chemical adsorption properties of penetrants in the zeolite.

Therefore, the purpose of this work is to combine the facilitated transport mechanism of noble metal ions with the molecular sieving mechanism of zeolites by a novel silver ion-exchange treatment of zeolite to improve the natural gas separation performance of MMMs. To our best knowledge, so far there is no academic literature available on using silver to conduct the ion-exchange treatment of zeolite for the application of MMMs in gas separations. Zeolite NaA before and after the silver ion-exchange treatment was used as the dispersed phase in this work because of its suitable pore size for natural gas separation. Polyethersulfone (PES) was chosen as the continuous polymer matrix because of its appropriate T_g of 215°C and various applications in gas separation.²⁴ Surface elements, crystal patterns, and total pore volume of zeolite NaA before and after the silver ion-exchange treatment were characterized by energy dispersion of X-ray (EDX), X-ray diffraction (XRD), and Brunauer–Emmett–Teller (BET) instruments, respectively. Flat dense PES–zeolite MMMs were fabricated based on a relatively straightforward approach by applying high processing temperatures during membrane formation.^{13,16,17} The gas permeation rates of flat dense PES–zeolite MMMs were measured as a function of zeolite loading. The morphology study of these developed MMMs was investigated by scanning electron microscopy (SEM).

Experimental

Materials

A commercial Radel A-300 PES (Amoco Performance Products Inc., Marietta, OH) was selected as the continuous phase in MMMs. It had a weight-average molecular weight of about 15,000 and was dried at 120°C overnight under vacuum before use. *N*-Methyl-2-pyrrolidone (NMP) was purchased from Merck (West Point, PA). NMP (>99%) was dried using the activated molecular sieve 4A; beads with a diameter of 0.003–0.005 m (3–5 mm) supplied by Research Chemicals Ltd. (Lancashire, U.K.) and then filtered through a 2×10^{-7} m (0.2 μ m) Teflon[®] filter before use. Zeolite NaA was supplied by UOP LLC (Des Plaines, IL). Its particle size varied from 1×10^{-6} m (1 μ m) to 2×10^{-6} m (2 μ m) tested by SEM. To remove the adsorbed water vapor or other organic vapors, all zeolites were dehydrated at 250°C for 7200 s (2 h) under vacuum before use. The silver nitrate solid was purchased from Merck and applied without further purification.

Silver ion-exchange treatment of zeolite NaA

After the preparation of 1×10^3 mol/m³ (1 mol/L) aqueous AgNO₃ solution, 1×10^{-3} kg (1 g) zeolite NaA was

added into $1 \times 10^{-4} \text{ m}^3$ (100 mL) aqueous AgNO_3 solution and then the solution was stirred for 3600 s (1 h) at 60–70°C in a temperature-controlled water bath. After the reaction, zeolite A with silver ion (designated zeolite AgA) was filtered and washed with $5 \times 10^{-4} \text{ m}^3$ (500 mL) deionized water to remove all the unreacted cations, and then was dried at 90°C overnight without vacuum. The resultant zeolite AgA was dehydrated using the above-mentioned procedure before use.

Preparation procedure of polymer–zeolite MMMs

Because the fabrication method of flat dense MMMs developed in our previous work has achieved good properties,²⁵ the same method was used in this work. We applied high processing temperatures during the membrane formation to eliminate or reduce the void formation between polymer and zeolite phases.

The resultant dried flat dense MMMs have thicknesses varying from $6 \times 10^{-5} \text{ m}$ (60 μm) to $7 \times 10^{-5} \text{ m}$ (70 μm) and a testing diameter of 0.02 m (2.0 cm) for permeability measurements.

Gas permeability measurement

Flat dense MMMs were tested in both pure gas and mixed gas systems in this work. Pure gas permeability was determined by a variable-pressure, constant-volume method described elsewhere.²⁶ The permeability of flat dense MMMs was obtained in the sequence of CH_4 and CO_2 at 35°C and $1.01325 \times 10^6 \text{ Pa}$ (10 atm). For the CO_2 -induced plasticization study, CO_2 permeation rates were tested with variable upstream pressures from $2.0265 \times 10^5 \text{ Pa}$ (2 atm) to $3.5464 \times 10^6 \text{ Pa}$ (35 atm) at a constant temperature of 35°C. The ideal selectivity of membranes for pure gases A to B is defined as follows:

$$\alpha_{A,B} = P_A/P_B \quad (1)$$

where P is the permeability of a membrane to a gas in $\text{m}^2 \text{ s}^{-1} \text{ Pa}^{-1}$ (1 Barrer = $1 \times 10^{-10} \text{ cm}^3 \text{ (STP)-cm/cm}^2\text{-s-cmHg} = 7.5005 \times 10^{-18} \text{ m}^2 \text{ s}^{-1} \text{ Pa}^{-1}$).

For mixed gas permeation measurements of flat dense MMMs, the pure gas permeation cell was modified.²⁷ The mixed gas testing system, a combination of permeation cell and gas chromatograph, allows the straightforward determination of gas permeability,²⁷ which is similar to the techniques used by O'Brien et al.²⁸ Each sample was tested at 35°C and $2.0265 \times 10^6 \text{ Pa}$ (20 atm) in a binary CO_2/CH_4 mixture (47/53% molar fraction). The selectivity of membranes for mixed gases A to B is defined as follows:

$$\alpha_{A,B} = \frac{(C_A/C_B)_{\text{permeate side}}}{(C_A/C_B)_{\text{feed side}}} \quad (2)$$

where C_A and C_B represent, respectively, molar fractions of gases A and B at the permeate and feed sides of the membrane.

Other characterizations

The elemental composition of zeolite surface before and after the silver ion-exchange treatment was measured by

Oxford Inca (Edinburgh, UK) energy dispersion of X-ray (EDX). The mapping mode was performed on the zeolite surface to detect the existence of certain elements, such as Na^+ and Ag^+ . XRD patterns of zeolite before and after the silver ion-exchange treatment were analyzed using a LabX-XRD 6000 X-ray diffractometer (XRD; Shimadzu, Kyoto, Japan) to quantitatively check the crystalline structure of zeolite at room temperature. The surface area and total pore volume of zeolites before and after the silver ion-exchange treatment were measured at 77 K on a high-speed gas-sorption analyzer (Model 3000 Series; Nova Analytical Systems, Niagara Falls, NY). The surface area of zeolites was determined through the standard multipoint BET method using nitrogen as the adsorbate. The total pore volume was derived from the amount of vapor adsorbed at a relative pressure close to unity by assuming that pores were then filled with liquid adsorbate.

The electron micrographs of flat dense MMM morphology were examined by SEM on JSM-5600LV and JSM-6700F equipment (JEOL, Tokyo, Japan) to determine whether the zeolite particles were distributed homogeneously and whether voids existed between polymer and zeolite phases. Samples for the cross-sectional characterization were fractured in liquid nitrogen. After mounting all the specimens on the stub by using double-sided conductive carbon adhesive tape, the specimens were further dried under vacuum overnight. All samples were sputter coated with platinum of $2\text{--}3 \times 10^{-8} \text{ m}$ (200–300 Å) in thickness using JEOL JFC-1200 ion-sputtering device before testing.

Results and Discussion

Characterization and comparison of zeolites NaA and AgA

To determine whether the silver ion-exchange treatment of zeolite is actually successful, measurement of the elemental composition of the zeolite surface before and after the silver ion-exchange treatment was performed by EDX instrument. EDX data shown in Table 1 demonstrate that sodium ion in zeolite NaA has been replaced completely by silver ion in the aqueous AgNO_3 solution after the ion-exchange treatment.

The crystalline properties of newly developed zeolite AgA were studied through XRD spectra. Figure 1 exhibits XRD patterns of zeolite A before and after the silver ion-exchange treatment. The XRD peak position and shape of zeolite AgA are essentially the same as those of zeolite NaA. In other

Table 1. Elemental Composition of Zeolite Surface before and after the Silver Ion Exchange Treatment Measured by EDX

Element	Atomic (%)	
	Before the Silver Ion Exchange Treatment	After the Silver Ion Exchange Treatment
O	64.8	63.2
Si	12.4	12.8
Al	11.3	11.9
Na	11.5	0.0
Ag	0.0	12.1
Total	100	100

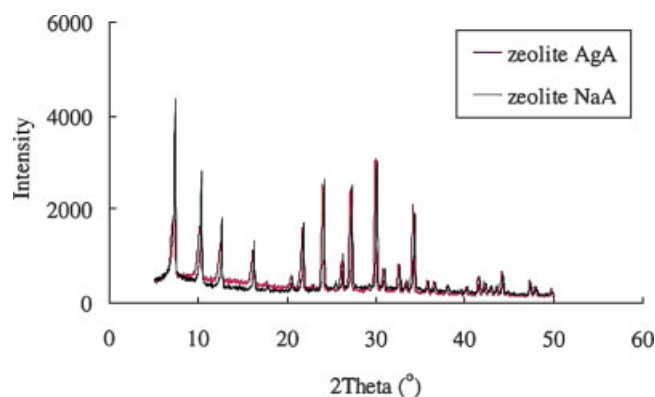


Figure 1. XRD patterns of zeolite A before and after the silver ion-exchange treatment.

[Color figure can be viewed in the online issue, which is available at www.interscience.wiley.com.]

words, zeolite AgA still possesses the crystallinity of zeolite NaA and, moreover, still maintains the intrinsic crystalline structure of zeolite NaA.

BET results shows that the total pore volume of zeolite NaA is $2.9 \times 10^{-4} \text{ m}^3/\text{kg}$ ($0.29 \text{ cm}^3/\text{g}$), whereas the ratio of total pore volume of zeolites AgA to NaA is 0.93. The reduction in the total pore volume after the silver ion-exchange treatment may be explained by the fact that the silver ionic radius of $1.15 \times 10^{-10} \text{ m}$ (1.15 \AA) is slightly larger than the sodium ionic radius of $1.02 \times 10^{-10} \text{ m}$ (1.02 \AA) and thus the pore size of zeolite AgA is slightly smaller than that of zeolite NaA. Therefore, we can conclude the porosity of zeolite is almost not compromised after the silver ion-exchange treatment.

Effect of silver ion-exchange treatment of zeolite on gas separation performance

Flat dense PES–zeolite A MMMs before and after the silver ion-exchange treatment of zeolite NaA were fabricated. Figure 2 shows their CO_2 and CH_4 permeability, whereas

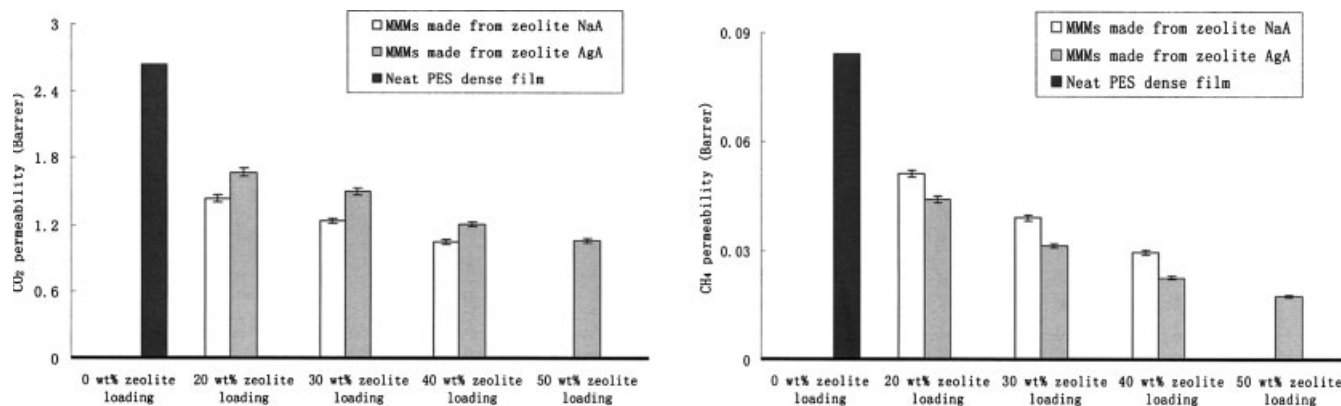


Figure 2. Comparison of CO_2 and CH_4 gas permeability of neat PES dense film and PES–zeolite A MMMs with two different metal forms.

1 Barrer = $7.5005 \times 10^{-18} \text{ m}^2 \text{ s}^{-1} \text{ Pa}^{-1}$.

Figure 3 summarizes their CO_2/CH_4 selectivity. Interestingly, the CO_2 permeability of MMMs made from zeolite AgA is higher than that of MMMs made from zeolite NaA at the same zeolite loading, whereas CH_4 permeability of MMMs made from zeolite AgA is lower than that of MMMs made from zeolite NaA. Cross-sectional SEM images of MMMs made from zeolites NaA and AgA shown in Figure 4 exhibit a similar zeolite distribution and contact between polymer and zeolite phases. Therefore, we may be able to rule out the change of interface properties as a possible cause for the opposite changing trend of CO_2 and CH_4 permeability after the silver ion-exchange treatment.

As we know, the pore size of zeolite AgA should be slightly smaller than that of zeolite NaA [that is, $3.8 \times 10^{-10} \text{ m}$ (3.8 \AA)] because the silver ionic radius is $1.15 \times 10^{-10} \text{ m}$ (1.15 \AA) and the sodium ionic radius is $1.02 \times 10^{-10} \text{ m}$ (1.02 \AA). The kinetic diameter of CH_4 gas molecule is just $3.8 \times 10^{-10} \text{ m}$ (3.8 \AA); therefore, the molecular sieving mechanism may be the primary reason why CH_4 permeability of MMMs made from zeolite AgA decreases. The kinetic diameter of CO_2 gas molecule is $3.3 \times 10^{-10} \text{ m}$ (3.3 \AA), which is smaller than the intrinsic pore sizes of zeolites NaA and AgA. Moreover, the double bond in CO_2 gas molecule can react reversibly with silver ion and form a π -bonded complex, thus facilitating the CO_2 gas molecule transport in zeolite AgA. The interaction of gases with the double bond and transition metals or their ions has been studied widely.^{29–32} The transition metals or their ions can form the normal σ -bond to carbon and, moreover, the unique characteristics of their d orbital can make them form bonds with unsaturated hydrocarbons in a nonclassical manner. For example, the work done by Takahashi et al.^{29,30} applied Ag ion-exchanged and Cu ion-exchanged zeolites for diene/olefin separation and exhibited excellent purification characteristics attributed to strong π -complexation bonds with CO and C_2H_4 . Kanazawa's work³¹ showed that C_2H_4 gas was barely adsorbed by zeolite ZSM5 because the molecules were too small; however, Ag ion-exchanged zeolite enabled C_2H_4 adsorption and, furthermore, the adsorption rate did not fall even at the high temperature of 500°C or after $3.6 \times 10^5 \text{ s}$ (100 h) durability testing. Therefore, the facilitated transport

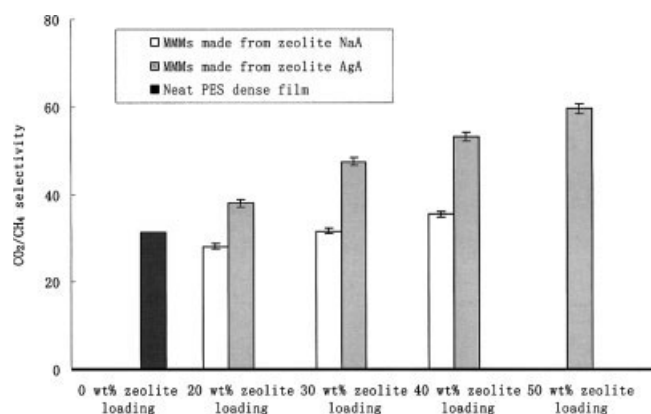


Figure 3. Comparison of CO₂/CH₄ selectivity of neat PES dense film and PES–zeolite A MMMs with two different metal forms.

mechanism may be a predominant reason why CO₂ permeability of MMMs made from zeolite AgA increases in our study.

The same reasons may be applicable to explain a CO₂/CH₄ selectivity increase when MMMs are made from zeolite AgA as illustrated in Figure 3. After the silver ion-exchange treatment of zeolite NaA, a combination of CO₂ permeability increase with CH₄ permeability decrease consequentially results in a significant improvement in CO₂/CH₄ selectivity

of MMMs made from zeolite AgA. In other words, two mechanisms—facilitated transport mechanism and molecular sieving mechanism—jointly lead to the remarkable enhancement in CO₂/CH₄ selectivity.

Effect of zeolite loadings on gas-separation performance

Flat dense PES–zeolite AgA MMMs with different zeolite loadings were fabricated. Neat PES dense films were also prepared with the same procedure for comparison. Their CO₂ and CH₄ permeability and CO₂/CH₄ selectivity at different zeolite loadings are also shown in Figures 2 and 3, respectively. The permeability of both gases decreases with an increase in zeolite content for PES–zeolite AgA MMMs. This decreasing trend of gas permeability with zeolite loading may be easily understandable because it was previously demonstrated that both polymer chain rigidification and partial pore blockage of zeolites may lead to a decrease in the gas permeability of MMMs.^{16,17,25} Although the π -bonded complex formed by a reversible reaction between CO₂ gas molecule and silver ion can facilitate the CO₂ gas molecule transport in zeolite AgA, the pore size of zeolite AgA is slightly smaller than 3.8×10^{-10} m (3.8 Å), which is very approximate to the kinetic diameter of CO₂ gas. Therefore, it can be concluded that the facilitated transport mechanism may not offset the negative effects of polymer chain rigidification and partial pore blockage of zeolites on CO₂ permeability.

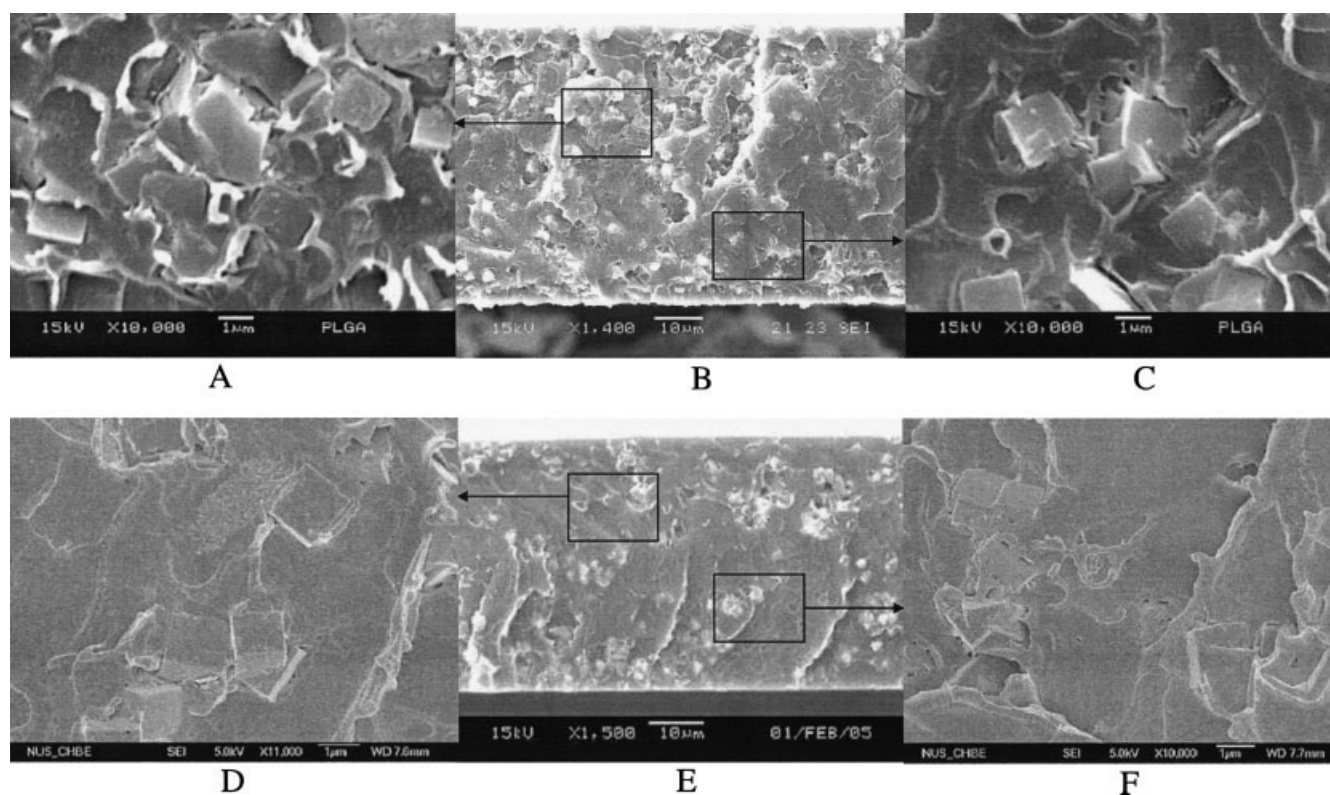


Figure 4. Comparison of cross-sectional SEM images of MMMs before and after the silver ion-exchange treatment.

A, B, C: PES–zeolite NaA MMMs; D, E, F: PES–zeolite AgA MMMs.

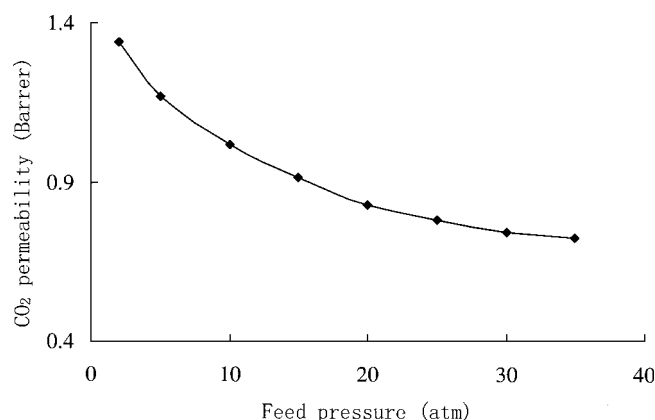


Figure 5. CO₂-induced plasticization testing results of PES-zeolite AgA MMMs at 50 wt % zeolite loading.

1 Barrer = $7.5005 \times 10^{-18} \text{ m}^2 \text{ s}^{-1} \text{ Pa}^{-1}$, 1 atm = $1.01325 \times 10^5 \text{ Pa}$.

Figure 3 also exhibits that CO₂/CH₄ selectivity of PES-zeolite AgA MMMs increases with an increase in zeolite loadings (from 31.4 at 0 wt % zeolite loading to 59.6 at 50 wt % zeolite loading). The highest increment reaches roughly 90% compared with that of neat PES dense film in the range of our study. This increasing trend of CO₂/CH₄ selectivity with an increase in zeolite loadings is also easily explainable as arising from the combined effect of the facilitated transport mechanism of silver ion and the molecular sieving mechanism of zeolite itself.

Applicability of PES-zeolite AgA MMMs in industry

To explore the applicability of newly developed PES-zeolite AgA MMMs in industry, this type of MMM with a 50 wt % zeolite loading was selected as a sample to carry out the CO₂-induced plasticization test and CO₂/CH₄ mixed gas measurement. Normally, gas permeability of membranes decreases with an increase in feed pressure resulting from the presence of unrelaxed volume in glassy polymers,¹⁶ whereas the CO₂-induced plasticization refers to an increase of CO₂ permeability as a function of feed pressure.^{33,34} As a plasticizer, CO₂ may either swell up the interstitial space among polymer chains, thus leading to a larger free volume, or/and enhance the mobility of segmental and side groups. Although the CO₂-induced plasticization accelerates the diffusion of penetrants in the membranes, simultaneously, it severely deteriorates CO₂/CH₄ permselectivity of membranes. Therefore, the effect of plasticization caused by CO₂ on the membrane separation performance should be avoided or diminished for a long-term and stable industrial application of membranes. Figure 5 shows the CO₂-induced plasticization testing results of PES-zeolite AgA MMMs at 50 wt % zeolite loading. It can be found that the plasticization does not occur even at the feed pressure of $3.5464 \times 10^6 \text{ Pa}$ (35 atm), which suggests that these newly developed PES-zeolite AgA MMMs possess high resistance to the CO₂-induced plasticization. The feed pressure here is nearly equal to the pressure difference over the membrane because the pressure in the permeate side of membranes is always not

higher than $1.3332 \times 10^3 \text{ Pa}$ (10 torr) during the test, which is negligible compared with high pressure (2.0265×10^5 – $3.5464 \times 10^6 \text{ Pa}$) in the feed side of membranes.

Normally, there may be some differences between pure gas and mixed gas separation performance. Possible reasons are the competition in sorption among the penetrants, the plasticization induced by CO₂ or hydrocarbon gases, the concentration polarization, and the nonideal gas behavior.^{35–37} Therefore, the mixed gas measurement is highly recommended to obtain true membrane separation performance in industrial applications. CO₂/CH₄ mixed gas with a 47/53% molar fraction was chosen as a separation object in this work. The mixed gas measurement results show that the PES-zeolite AgA MMM at 50 wt % zeolite loading possesses CO₂ permeability of $8.6256 \times 10^{-18} \text{ m}^2 \text{ s}^{-1} \text{ Pa}^{-1}$ (1.15 Barrer) and CO₂/CH₄ selectivity of 58.1. By comparing with pure gas separation performance shown in Figures 2 and 3, it can be seen that the difference between mixed gas and pure gas separation performance is almost negligible, which indicates that these newly developed PES-zeolite AgA MMMs still can maintain a high performance even in mixed gas separation.

Experimental results from both CO₂-induced plasticization test and CO₂/CH₄ mixed gas measurement demonstrate that PES-zeolite AgA MMMs developed in this work are a type of potential and excellent membrane material for natural gas separation in industrial applications. Although CO₂ permeability of PES-zeolite AgA MMMs developed in this work is relatively low compared with that of commercial polymer membranes, this problem can be solved by using other polymer materials with a high intrinsic CO₂ permeability as the matrix of MMMs or/and applying this type of PES-zeolite AgA composite membrane material in the configuration of hollow fibers with an ultrathin dense-selective layer and a large surface area per unit volume. These will be the focus of systematic investigations in our future work.

Conclusions

The following conclusions can be drawn from this work:

1. EDX data demonstrate that sodium ion in zeolite NaA has been replaced completely by silver ion in an aqueous AgNO₃ solution after the ion-exchange treatment. XRD patterns show that zeolite AgA still possesses the crystallinity of zeolite NaA and maintains the intrinsic crystalline structure of zeolite NaA. BET results indicate that the porosity of zeolite is almost not compromised after the silver ion-exchange treatment. These three characterizations ensure zeolite AgA is a good candidate that can be applied in the fabrication of MMMs.

2. Compared with the natural gas separation performance of PES-zeolite NaA MMMs, a decrease in CH₄ permeability of PES-zeolite AgA MMMs may primarily result from the reduction of zeolite pore size after the silver ion-exchange treatment, whereas an increase in CO₂ permeability may be predominantly attributable to the facilitated transport mechanism between silver ion and CO₂ gas molecule. Consequently, a significantly enhanced CO₂/CH₄ selectivity is obtained through PES-zeolite AgA MMMs.

3. CO₂ and CH₄ permeability of PES-zeolite AgA MMMs decreases with increasing zeolite content. Clearly, the facili-

tated transport mechanism may not offset the negative effects of polymer chain rigidification and partial pore blockage of zeolites on CO₂ permeability because the pore size of zeolite AgA is very close to the kinetic diameter of CO₂ gas. CO₂/CH₄ selectivity of PES–zeolite AgA MMMs increases with an increase in zeolite loadings and the highest value reaches 59.6 at 50 wt % zeolite loading as the result of a combined effect of the facilitated transport mechanism of silver ion and the molecular sieving mechanism of zeolite itself.

4. These newly developed PES–zeolite AgA MMMs exhibit high resistance to the CO₂-induced plasticization and show comparable CO₂ and CH₄ permeability and CO₂/CH₄ selectivity in both pure gas and mixed gas permeation rate measurements, which demonstrate that these MMMs are a type of potential and excellent membrane material for natural gas separation in industrial applications.

Acknowledgments

The authors thank UOP LLC and NUS for funding this research (Grants R-279-000-140-592, R-279-000-140-112, and R-279-000-184-112). We thank Dr. Huang for aiding in the silver ion-exchange treatment of zeolite NaA.

Literature Cited

- Paul DR, Yampol'skii YP. *Polymeric Gas Separation Membranes*. Boca Raton, FL: CRC Press; 1994.
- Koros WJ, Fleming GK. Membrane-based gas separation. *J Membr Sci*. 1993;83:1–80.
- Staudt-Bickel C, Koros WJ. Improvement of CO₂/CH₄ separation characteristics of polyimides by chemical crosslinking. *J Membr Sci*. 1999;155:145–154.
- Tabe-Mohammadi A. A review of the applications of membrane separation technology in natural gas treatment. *Sep Sci Technol*. 1999;34:2095–2111.
- Robeson LM. Correlation of separation factor versus permeability for polymeric membranes. *J Membr Sci*. 1991;62:165–185.
- Teramoto M, Matsuyama H, Yamashiro T, Katayama Y. Separation of ethylene from ethane by supported liquid membranes containing silver nitrate as a carrier. *J Chem Eng Jpn*. 1986;19:419–424.
- Ho WS, Dalrymple DC. Facilitated transport of olefins in Ag⁺-containing polymer membranes. *J Membr Sci*. 1994;91:13–25.
- Yang JS, Hsiue GH. Selective olefin permeation through Ag(I) contained silicone rubber-graft-poly(acrylic acid) membranes. *J Membr Sci*. 1997;126:139–149.
- Barsema JN, Balster J, Jordan V, van der Vegt NFA, Wessling M. Functionalized carbon molecular sieve membranes containing Ag-nanoclusters. *J Membr Sci*. 2003;219:47–57.
- Kulprathipanja S, Neuzil RW, Li NN. *Separation of Fluids by Means of Mixed Matrix Membranes in Gas Permeation*. U.S. Patent No. 4 740 219; 1988.
- Te Hennepe HJC. *Zeolite Filled Polymeric Membranes: A New Concept in Separation Science*. PhD Thesis. Enschede, The Netherlands: University of Twente; 1988.
- Jia MD, Peinemann KV, Behling RD. Molecular sieving effect of the zeolite-filled silicone rubber membranes in gas permeation. *J Membr Sci*. 1991;57:289–296.
- Mahajan R, Burns R, Schaeffer M, Koros WJ. Challenges in forming successful mixed matrix membranes with rigid polymeric materials. *J Appl Polym Sci*. 2002;86:881–890.
- Duval JM, Kemperman AJB, Folkers B, Mulder MHV, Desgrand-champs G, Smolders CA. Preparation of zeolite filled glassy polymer membrane. *J Appl Polym Sci*. 1994;54:409–418.
- Yong HH, Park HC, Kang YS, Won J, Kim WN. Zeolite-filled polyimide membrane containing 2,4,6-triaminopyrimidine. *J Membr Sci*. 2001;188:151–163.
- Mahajan R. *Formation, Characterization and Modeling of Mixed Matrix Membrane Materials*. PhD Dissertation. Austin, TX: The University of Texas; 2000.
- Li Y, Guan HM, Chung TS, Kulprathipanja S. Effects of novel silane modification of zeolite surface on polymer chain rigidification and partial pore blockage in polyethersulfone (PES)-zeolite A mixed matrix membranes. *J Membr Sci*. 2006;275:17–28.
- McDaniel CV, Mayer PK. Molecular sieves. *Soc Chem Ind Monogr*. 1968.
- Flanigen EM. Molecular sieve zeolite technology: The first twenty-five years. *Pure Appl Chem*. 1980;52:2191–2211.
- Derouane EG. *Zeolite Microporous Solids: Synthesis, Structure, and Reactivity*. Dordrecht, The Netherlands: Kluwer Academic; 1992.
- Taizo K, Tooru N, Isao T, Wataru I. *Manufacture of Zeolite 3A from Zeolite 4A*. European Patent No. JP5147926; 1993.
- Heide W. *Production of Acid-modified Potassium Zeolite 3A by Cation Exchange of Sodium Zeolite 4A*. European Patent No. DE10107819; 2002.
- Guan HM, Chung TS, Huang Z, Chng ML, Kulprathipanja S. Poly(vinyl alcohol) multilayer mixed matrix membranes for the dehydration of ethanol-water mixture. *J Membr Sci*. 2006;268:113–122.
- Chiou JS, Maeda Y, Paul DR. Gas permeation in polyethersulfone. *J Appl Polym Sci*. 1987;33:1823–1828.
- Li Y, Chung TS, Cao C, Kulprathipanja S. The effects of polymer chain rigidification, zeolite pore size and pore blockage on polyethersulfone (PES)-zeolite A mixed matrix membranes. *J Membr Sci*. 2005;260:45–55.
- Lin WH, Vora RH, Chung TS. Gas transport properties of 6FDA-Durene/1,4-phenylenediamine (pPDA) copolyimides. *J Polym Sci Part B: Polym Phys*. 2000;38:2703–2713.
- Tin PS, Chung TS, Liu Y, Wang R, Liu SL, Pramoda KP. Effects of cross-linking modification on gas separation performance of Matrimid membranes. *J Membr Sci*. 2003;225:77–90.
- O'Brien KC, Koros WJ, Barbari TA, Sanders ES. A new technique for the measurement of multicomponent gas transport through polymer films. *J Membr Sci*. 1986;29:229–238.
- Takahashi A, Yang RT, Munson CL, Chinn D. Influence of Ag content and H₂S exposure on 1,3-butadiene/1-butene adsorption by Ag ion-exchanged Y-zeolites (Ag-Y). *Ind Eng Chem Res*. 2001;40:3979–3988.
- Takahashi A, Yang RT, Munson CL, Chinn D. Cu(I)-Y-zeolite as a superior adsorbent for diene/olefin separation. *Langmuir*. 2001;17:8405–8413.
- Kanazawa T. Development of hydrocarbon adsorbents, oxygen storage materials for three-way catalysts and NO_x storage-reduction catalyst. *Catal Today*. 2004;96:171–177.
- Matsuoka M, Iino K, Chen HJ, Anpo M. Local structures of Ag (I) clusters prepared within zeolites by ion-exchange method and their photochemical properties. *Res Chem Intermed*. 2005;31:153–165.
- Bos A, Punt IGM, Wessling M, Strathmann H. CO₂-induced plasticization phenomena in glassy polymers. *J Membr Sci*. 1999;155:67–78.
- Ismail AF, Lorna W. Penetrant-induced plasticization phenomenon in glassy polymers for gas separation membrane. *Sep Purif Technol*. 2002;27:173–194.
- Raymond PC, Koros WJ, Paul DR. Comparison of mixed and pure gas permeation characteristics for CO₂ and CH₄ in copolymers and blends containing methyl methacrylate units. *J Membr Sci*. 1993;77:49–57.
- Coleman MR, Koros WJ. Conditioning of fluorine-containing polyimides. 2. Effect of conditioning protocol at 8% volume dilation on gas-transport properties. *Macromolecules*. 1999;32:3106–3113.
- Kim JH, Ha SY, Lee YM. Gas permeation of poly(amide-6-b-ethylene oxide) copolymer. *J Membr Sci*. 2001;190:179–193.

Manuscript received Jun. 14, 2006; revision received Sept. 15, 2006, and final revision received Dec. 18, 2006.